Editorial Manager(tm) for Applied Composite Materials
Manuscript Draft

Manuscript Number:

Title: POST-IMPACT MECHANICAL CHARACTERISATION OF GLASS AND BASALT WOVEN FABRIC LAMINATES

Article Type: Original Research

Keywords: Basalt; E-glass; acoustic emission; residual properties; impact

Corresponding Author: Carlo Santulli, PhD

Corresponding Author's Institution: Università di Roma La Sapienza

First Author: Igor M. De Rosa, PhD

Order of Authors: Igor M. De Rosa, PhD;Francesco Marra, PhD;Giovanni Pulci, PhD;Carlo Santulli, PhD;Fabrizio Sarasini, PhD;Jacopo Tirillò, PhD;Marco Valente, PhD

Abstract: Two woven fabric laminates, one based on basalt fibres, the other on E-glass fibres, as a reinforcement for vinylester matrix, were compared in terms of their post-impact performance. With this aim, first the non-impacted specimens were subjected to interlaminar shear stress and flexural tests, then flexural tests were repeated on laminates impacted using a falling weight tower at three impact energies (7.5, 15 and 22.5 J). Tests were monitored using acoustic emission analysis of signal distribution with load and with distance from the impact point. The results show that the materials have a similar damage tolerance to impact and also their post-impact residual properties after impact do not differ much, with a slight superiority for basalt fibre reinforced laminates. The principal difference is represented by the presence of a more extended delamination area on E-glass fibre reinforced laminates than on basalt fibre reinforced ones.

POST-IMPACT MECHANICAL CHARACTERISATION OF GLASS AND BASALT WOVEN FABRIC LAMINATES

Igor M. De Rosa, Francesco Marra, Giovanni Pulci, Carlo Santulli, Fabrizio Sarasini, Jacopo Tirillò, Marco Valente

Sapienza - Università di Roma
Department of Chemical Engineering Materials Environment
Via Eudossiana 18 - 00184 Rome, Italy

Abstract

Two woven fabric laminates, one based on basalt fibres, the other on E-glass fibres, as a reinforcement for vinylester matrix, were compared in terms of their post-impact performance. With this aim, first the non-impacted specimens were subjected to interlaminar shear stress and flexural tests, then flexural tests were repeated on laminates impacted using a falling weight tower at three impact energies (7.5, 15 and 22.5 J). Tests were monitored using acoustic emission analysis of signal distribution with load and with distance from the impact point. The results show that the materials have a similar damage tolerance to impact and also their post-impact residual properties after impact do not differ much, with a slight superiority for basalt fibre reinforced laminates. The principal difference is represented by the presence of a more extended delamination area on E-glass fibre reinforced laminates than on basalt fibre reinforced ones.

INTRODUCTION

In recent years, natural fibres are increasingly proposed as an alternative to glass fibres as a result of stricter environmental requirements. Natural fibres may either be extracted from plants, such it is the case for jute, flax, hemp, etc., or have a mineral origin: among the latter, basalt fibres appear at the moment to be the most popular ones. With respect to other environmentally friendly materials, such as plant fibres, which equally show thermal and acoustic insulation properties, the higher specific weight of basalt fibres (about 2700 kg/m^3) is widely compensated by their higher modulus, excellent heat resistance, good resistance to chemical attack and low water absorption [1]. This suggests the possibility to apply them as a replacement for glass fibres, also because their chemical composition is not very different, since continuous basalt fibre has a not very different content in silica and alumina from glass fibres and therefore a comparable, if not superior, tensile strength [2].

Basalt fibres appear therefore suitable in principle to be applied as reinforcement for composite materials: on this possibility a number of studies exist, in particular using thermoplastic [3–6] and thermosetting matrices [7–9]. Most of these papers deal with short basalt fibres and few papers are concerned with woven fabrics [10–13]. Some of the aforementioned studies on basalt fibre composites involved some use of the acoustic emission (AE) technique to monitor mechanical behaviour of the laminates [7-8]. In particular, their main objectives were a multi-parameter AE study during tensile tests [7] and the use of amplitude distribution for damage characterization and of AE localisation for crack propagation studies [8].

A previous study was aimed at the comparison and discussion of the mechanical and electrical properties of composites reinforced with basalt and E-glass woven fabrics, both characterized by the same weave pattern, to assess the suitability of basalt fabrics as an effective contender of glass fabrics for the reinforcement of composites [14]. This appears to be further confirmed by a recent comparative study between basalt and E-glass woven composites, where the former showed higher Young's modulus, compressive and flexural strength, whilst the latter exhibited a higher tensile strength, with the limitation that a lower areal weight was used for basalt fabric [15].
Moreover, in the case of composites to be used in structural components, other issues arise, in particular the need to provide sufficient impact resistance. A recent study investigating low velocity impact behaviour of laminates reinforced by basalt fabrics, as compared with nylon-basalt hybrid laminates, suggested that their major energy absorption mechanism is fibre breakage, rather than delamination [16]. If confirmed, this would imply that their mode of fracture under impact loading would be different from that of glass fibre composites, a point which would suggest the usefulness of a comparative study between the two materials as regards their impact behaviour, possibly with the support of other characterisation methods, such as non destructive techniques.

In this study, the material is fully characterised using interlaminar shear strength tests and flexural tests. Impact damage is characterised from the study of post-impact flexural properties assisted by acoustic emission and thermography, visualising damage using scanning electron microscope (SEM) fractographs, along the lines of what has been carried out in two comparative studies between configurations of glass/jute fibre hybrid laminates, performed by the same research group [17-18].

MATERIALS AND METHODS

The basalt (BAS 220.1270.P) and E-glass fabrics (RE 220P) were plain weave fabrics supplied by Basaltex-Flocart NV (Belgium) and Mugnaini Group srl (Italy), respectively. Both fabrics were characterized by the same specific surface weight, namely 220 g/m^2. The matrix used was a Bisphenol-A epoxy based vinylester resin (DION 9102) produced by Reichhold, Inc (USA). The hardener and accelerator were Butanox LPT (MEKP, 2wt.%) and NL-51P (Cobalt 2-ethylhexanoate, 1wt.%), respectively. The laminates were manufactured by a laboratory Resin Transfer Moulding (RTM) system [14]. From the laminates were cut the specimens for the mechanical characterization. The same number of fabrics was used, and the fibre volume fraction for both composites was similar and equal to 0.38 ± 0.02. Four-point bending tests were performed in accordance with ASTM D 6272. Five specimens for each composite type were tested, having the following dimensions: 150 mm × 30 mm × 3.1 mm (L×W×t). A span-to-depth ratio of 25:1 and a cross-head speed of 2.5 mm/min were used. Strain gauges were used to evaluate the flexural modulus. The interlaminar shear strength was evaluated in accordance with ASTM D 2344. Ten specimens were tested for each laminate, having the following dimensions: 20 mm × 6.2 mm × 3.1 mm (L×W×t). A span-to-depth ratio of 4:1 and a cross-head speed of 1 mm/min were used. The mechanical characterization was performed on a Zwick/Roell Z010 universal testing machine equipped with a 10 kN load cell.

The specimens from glass and basalt laminates were impacted and then subjected to post-impact four-point bending tests. The impact point was located at the centre of the specimens. The impact energy was changed varying the mass of the hemispherical drop-weight striker (φ = 12.7 mm), thus keeping a constant velocity of 2.5 m/s. Impact tests were performed on an instrumented impact tower fitted with an anti-rebound device. Three different impact energies were considered: 7.5, 15 and 22.5 J. Post-impact bending tests were performed using the same parameters previously described.

Post-impact flexural tests were monitored by acoustic emission until final fracture occurred using an AMSY-5 AE system by Vallen Systeme GmbH (Germany). The AE acquisition settings used throughout this experimental work were as follows: threshold = 35 dB, Rearm Time (RT) = 0.4 ms, Duration Discrimination Time (DDT) = 0.2 ms and total gain = 34 dB. The PZT AE sensors used (Deci, SE150-M) were resonant at 150 kHz. The sensors were placed on the surface of the specimens at both ends to allow linear localization.

After impact, the damaged area was observed using an Avio/Hughes Probeye TVS 200 thermal video system. The heating was obtained using a 500W lamp: a 5 s pulse was applied, positioning

the lamp at approximately 200 mm from the sample, so that a maximum temperature of 35°C was obtained on the sample surface. The cooling transient period was not so long to allow images acquisition, so that the thermograms were acquired between 2 and 5 s during heating. The emissivity was set at 0.90 for basalt and at 0.15 for glass reinforced laminates, since this value offered in both cases the image with the best contrast with the background. The variations of temperature on the specimen surface were mainly ascribed to geometry alterations produced by impact damage, since both these composites show poor conductivity.

The microstructural characterization was carried out by scanning electron microscopy (SEM) using a Philips XL40. Prior to all SEM observations, the specimens were sputtered with gold to prevent charging.

RESULTS AND DISCUSSION

Mechanical tests

Non-impacted basalt fibre reinforced laminates show mechanical properties which are slightly superior to those of E-glass fibre reinforced laminates: this is visible from ILSS tests (Figure 1), and from flexural strength and modulus (Figure 2 and 3, respectively).

As regards the degradation of flexural properties with increasing impact energies, this appears to be not very different between the two laminates (see again Figure 2 and 3). The residual flexural strength of impact damaged specimens normalized to that of undamaged ones (figure 4) shows a sharper reduction in the case of glass reinforced composites for impact energies exceeding 7.5 J, thus pointing out a better damage tolerance capability for basalt laminates. The decrease in flexural stiffness follows a similar pattern in both laminates, even though a slightly better behaviour for glass fibre laminates was observed. As a consequence, basalt fibre laminates do retain their superiority in absolute terms, showing even a lower degradation in terms of flexural strength at the higher impact energies, 15 and 22.5 J.

In general, this is not a surprising result, as it confirms some recent work on E-glass and basalt fibre reinforced laminates, which suggested that basalt fibre reinforcement has improved strength properties in a range of loading scenarios over E-glass fibre laminates [19]. Damage evolution during loading, especially of already impacted basalt fibre laminates, need further clarification, which may be supplied by real time acoustic emission monitoring during loading.

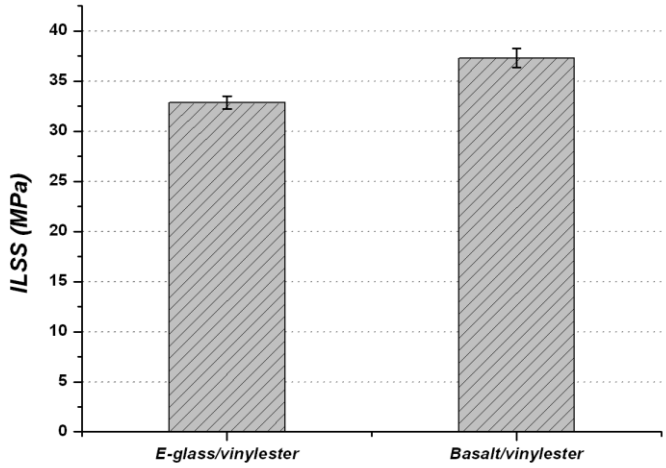

Figure 1 Interlaminar shear strength of the two laminates

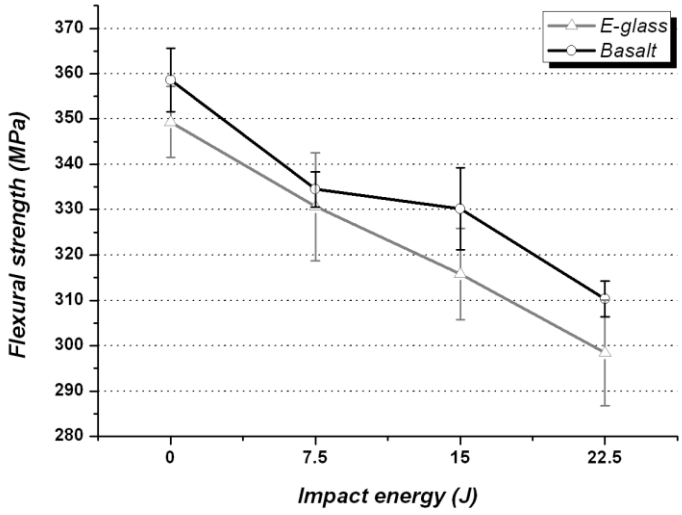

Figure 2 Post-impact flexural strength of the two laminates

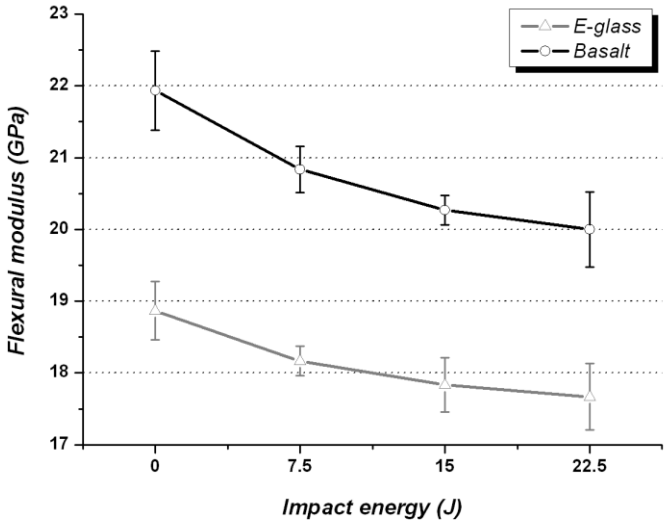

Figure 3 Post-impact flexural modulus of the two laminates

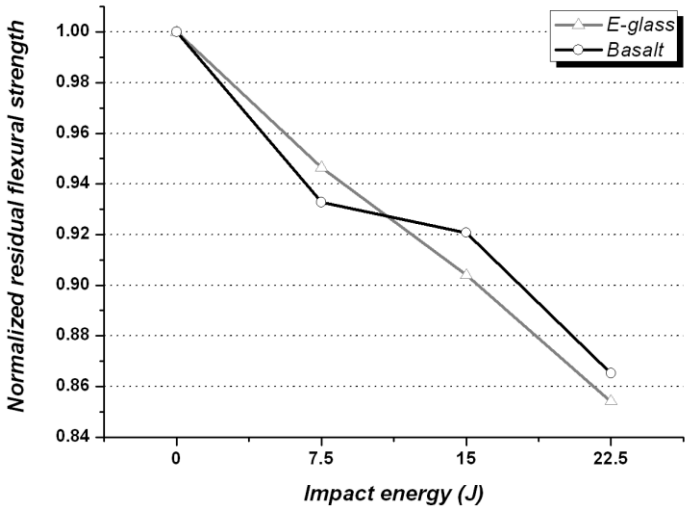

Figure 4 Normalised residual flexural strength of the two laminates

Acoustic emission analysis

As a preliminary consideration, from AE cumulative counts vs. time curves, it is possible to identify an approximate load when acoustic emission activity starts. In particular, acoustic emission is considered to commence, apart from sparse low-counts events, which may take place even at very low load, when it starts to be visible from the global AE cumulative counts vs. time graphs, an example of which is given in Figure 5. This happens when AE counts exceed approximately 1/500 of the final cumulative counts: at this point, an AE start load is measured. This derives empirically

from the maximum achievable end-of-scale of the graph on the Y-axis (1654 pixels), and the fact that only a gradient of not less than three pixels starts to be visible.

Above the AE start load, AE activity during monotonic loading is likely to grow with increasing stress, although the specific characteristics of such behaviour may change considerably depending on materials properties and presence of irreversible damage. To better clarify these characteristics, the tests have been divided in five phases, according to the load levels, from 0 to 25%, 25 to 50%, 50 to 75%, and 75 to 100% of the maximum load. The fifth phase is denominated as "post" and represents those AE events detected after reaching the maximum load, when the load decreases in the immediate proximity of failure. The phases are reported on a typical flexural loading curve in Figure 6.

A further analysis of AE data is performed on their location with respect to impact (if any): the centre of the impacting head corresponds to the midpoint between the edge of the two sensors (located at abscissa 15 and 135 mm, respectively), at the abscissa x=75 mm. With respect to their locations, the events are divided in four classes, namely A, for those detected within the impacted length (68-81 mm), B, detected in a location displaced by no more than one impacted length from either of the extremes of A (55-68 and 81-94 mm), C, detected in the remaining part of the laminate between the sensor edges (15-55 and 94-135 mm), and D, detected under the sensors and outside them (0-15 and 135-150 mm).

More specifically, the localisation analysis is aimed at discerning on impacted samples between the two principal modes of impact damage. These are the indentation mode, which is limited to the area in physical contact with the impacting head ("A" class of AE events), and the delamination mode, which has been approximated for low impact energies with a ring-shaped area extending no further than twice the impacting head diameter from the centre ("B" class of AE events). Other events detected in the bulk of the laminate between the sensors are in the "C" class, whilst those very close to the laminate's edge, which can be supposed to be mostly unrelated with fracture events are in the "D" class. An example of the distribution between the four classes is reported using different colours in Figure 7.

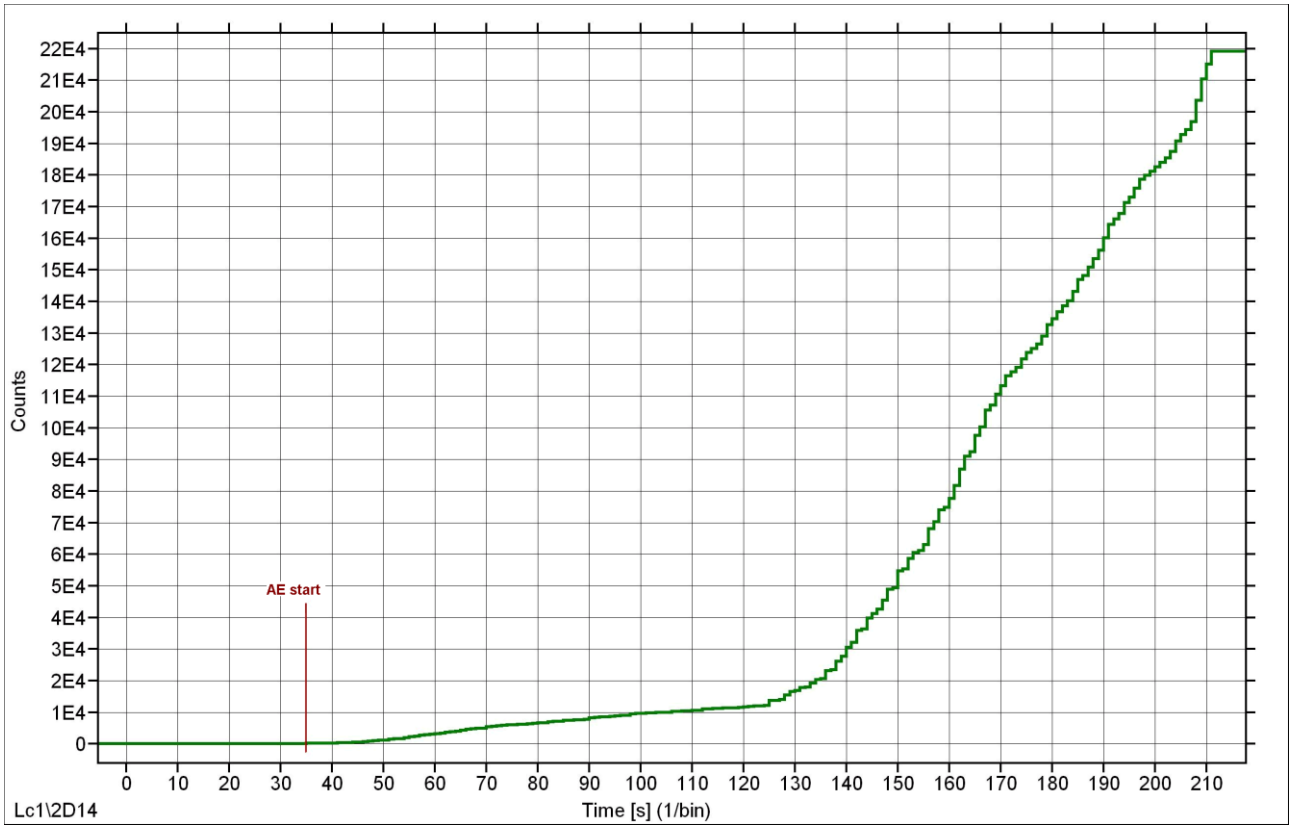

Figure 5 AE start load measured from cumulative counts vs. time curve

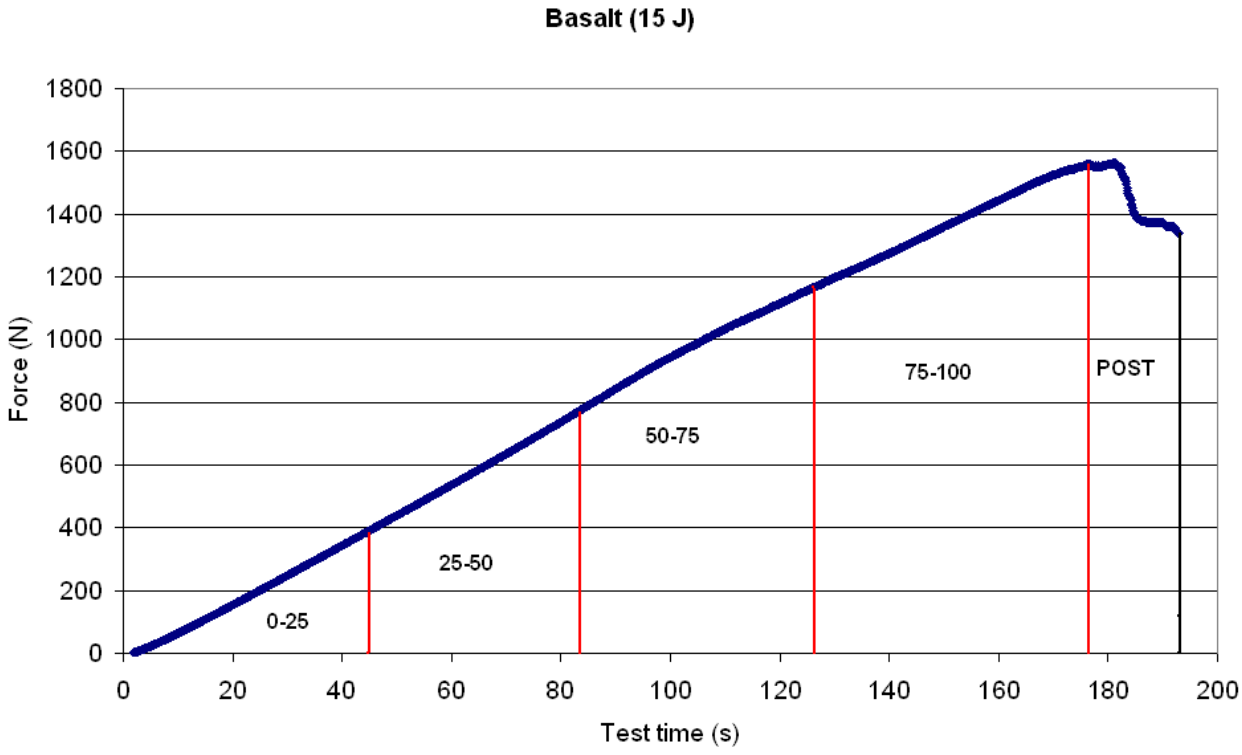

Figure 6 Load levels on a typical flexural load vs. time curve

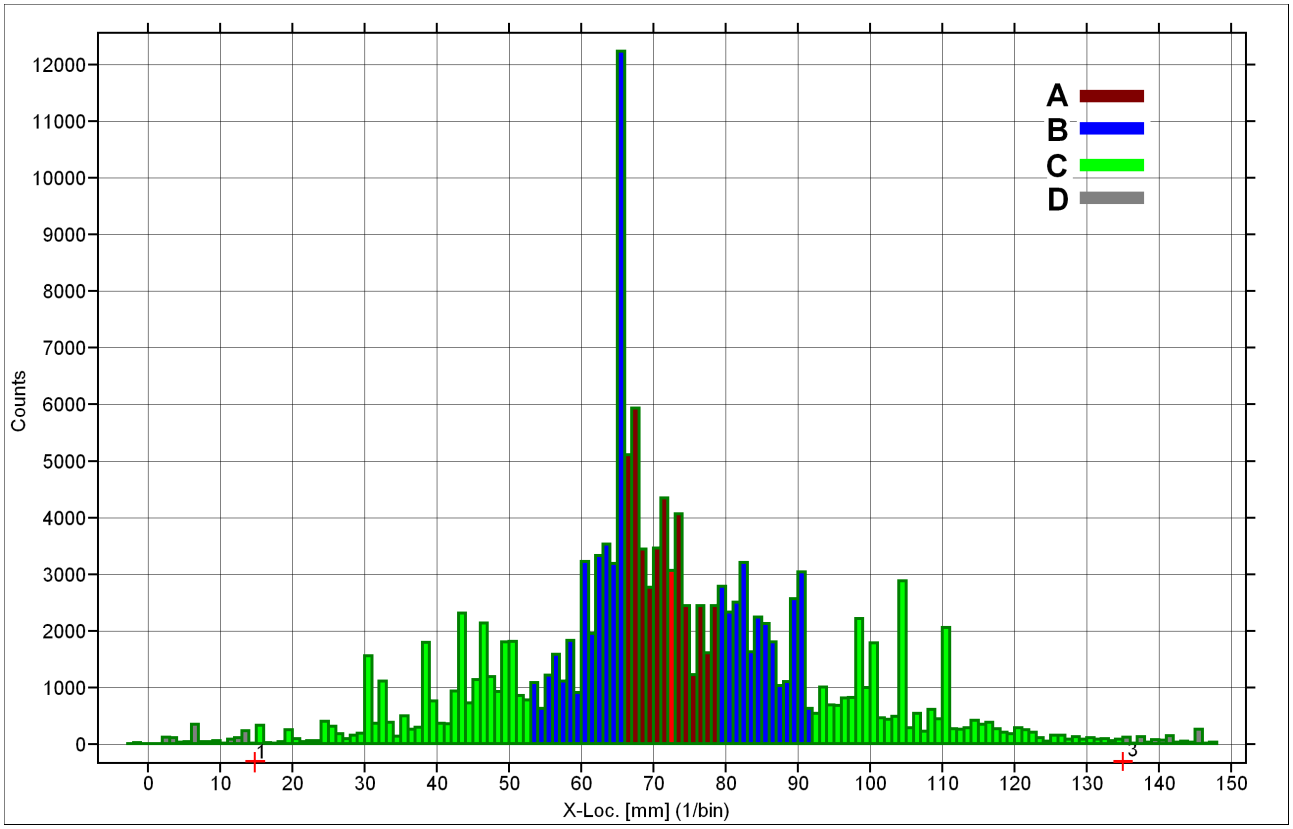

Figure 7 Partition of the events according to their location along the laminate (on a basalt fibre reinforced laminate impacted at 22.5 J)

In Figure 8a and 8b the AE start stress of basalt and glass fibre reinforced laminates is reported, respectively. The average value of AE start stress for the former is slightly superior to that of the latter, except for the laminates impacted at the maximum energy, 22.5 J. The significance of this indication is somehow reduced by the presence of a large scattering between values.

The growth of acoustic emission with load is the expected trend in Figure 9a and 9b, for the simple consideration that the occurrence of irreversible damage is likely to grow with applied stress. However, it is to be noted that in impacted laminates some damage has been introduced already, the presence of which may conceal the increasing trend of damage progression. Here, in basalt fibre reinforced laminates acoustic emission does not appear to grow steadily with load between 25% and the maximum stress, while in absolute terms the count rate over time value is higher than in glass fibre reinforced laminates, in particular between 25 and 50% of the maximum stress. This may indicate an earlier occurrence of irreversible damage, possibly connected with the significant presence of fractured fibres, as suggested in [16]. On the other side, the limited progression of damage with increasing load may indicate the better damage tolerance of basalt fibre composites.

AE localisation analysis (Figure 10a and 10b) suggests that for the maximum impact energy both laminates show an increased concentration of events in the impact area (A class events). In contrast,

for non-impacted basalt fibre reinforced laminates there is little difference in the count rate over distance of A, B and C class events, whilst some preference for A and B events with respect to C ones can be noted on impacted glass fibre reinforced laminates. The comparison between the two laminates appears also to indicate that delamination mode (B events) is definitely prevalent over indentation mode (A events) for 7.5 and 15 J impacted laminates on basalt fibre reinforced composites, whilst this is less evident for glass fibre reinforced ones. In contrast, for both laminates impacted at 22.5 J, indentation mode becomes slightly prevalent over delamination one. In general, it may be concluded that the differences between the two laminates in terms of AE localisation analysis are not very large.

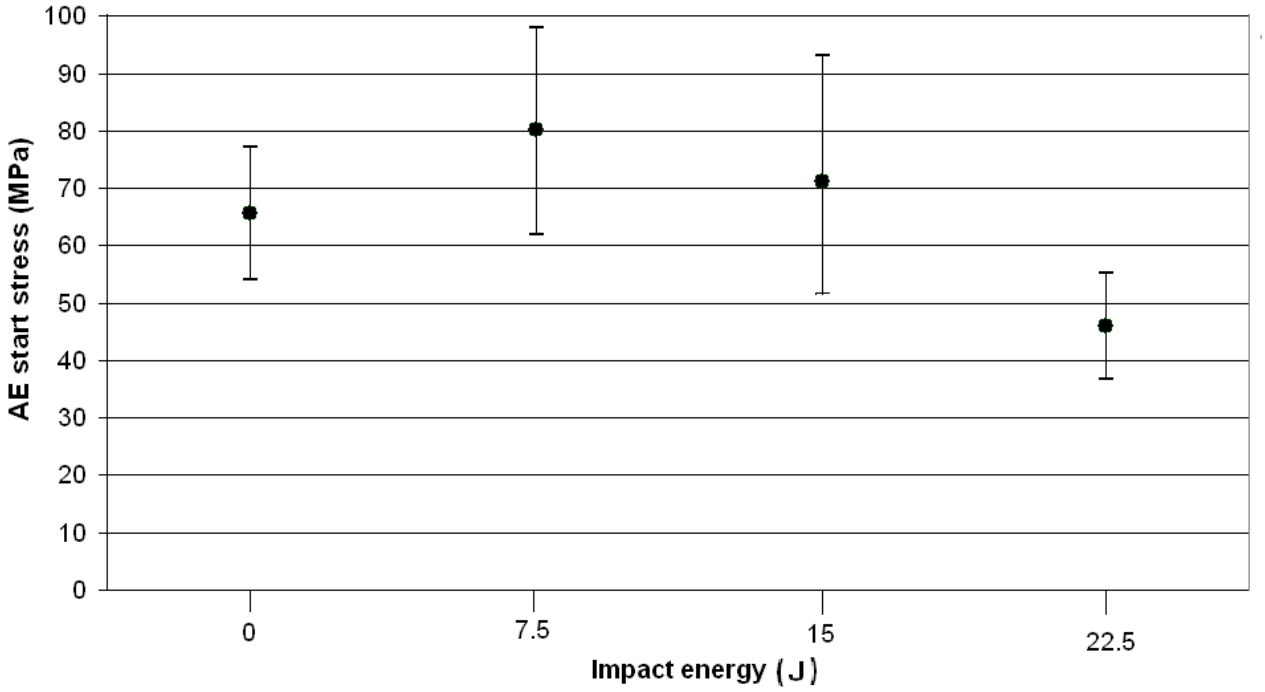

Figure 8a AE start stress (MPa) vs. impact energy (J) for basalt fibre reinforced laminates

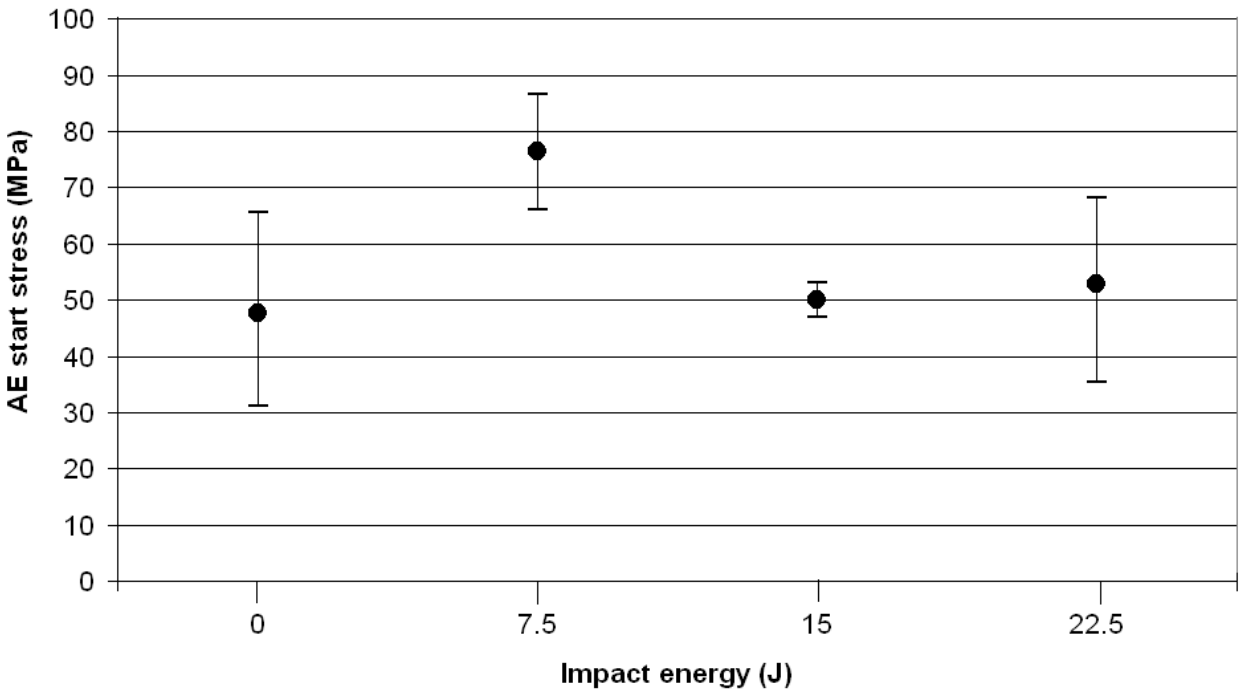

Figure 8b AE start stress (MPa) vs. impact energy (J) for E-glass fibre reinforced laminates

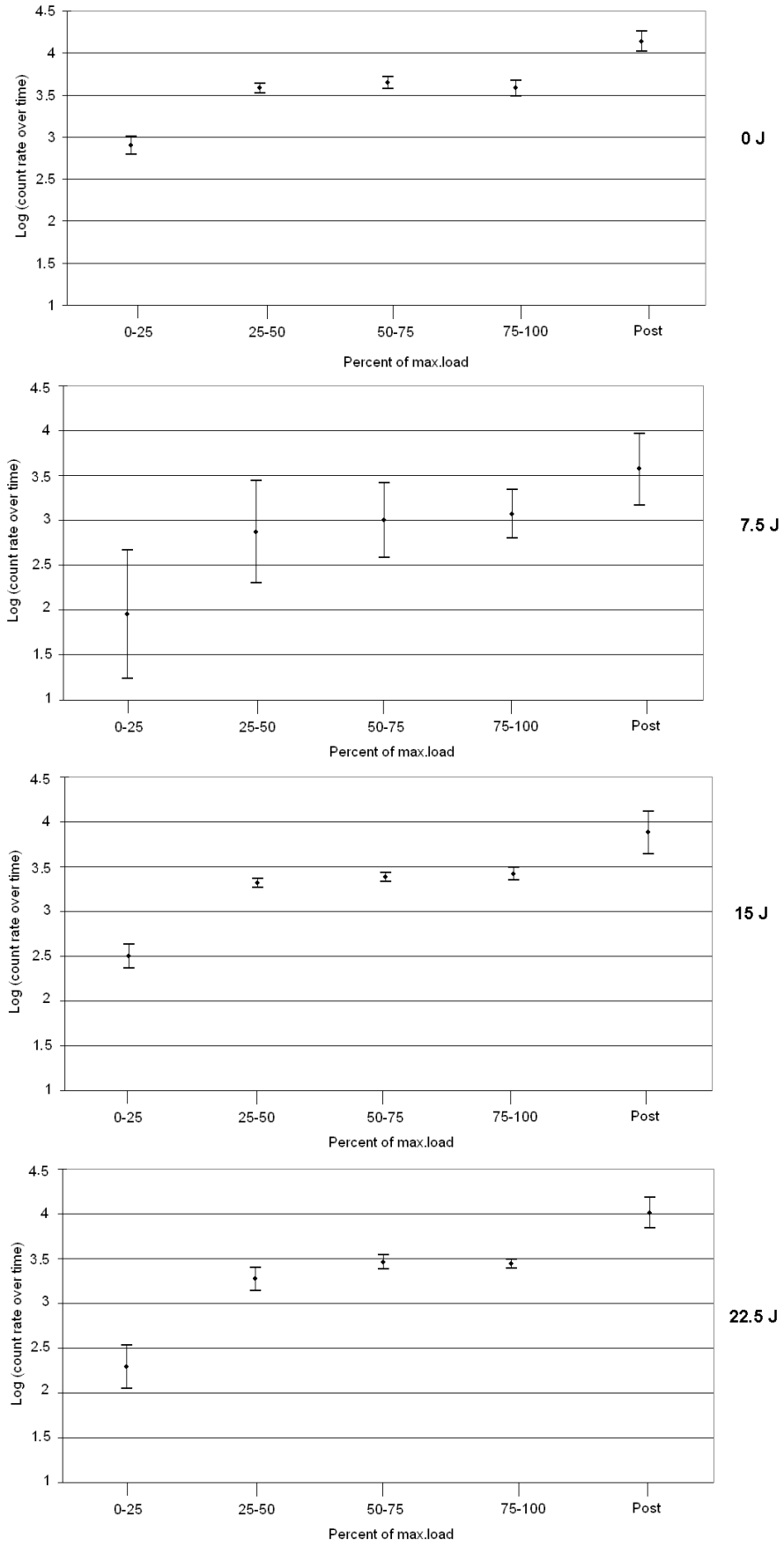

Figure 9a AE log (Count rate over time) vs. load for basalt fibre reinforced laminates

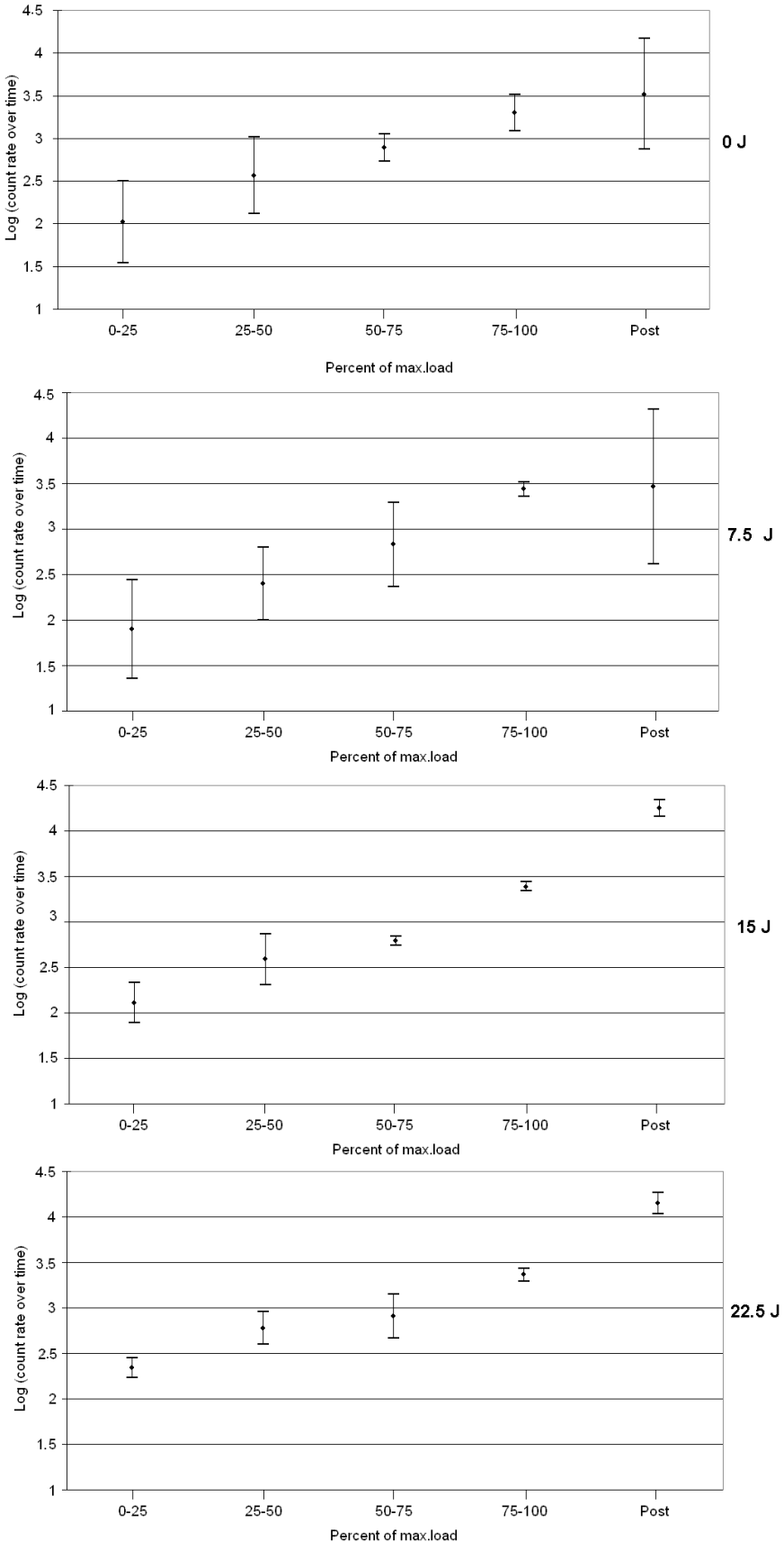

Figure 9b AE log (Count rate over time) vs. load for E-glass fibre reinforced laminates

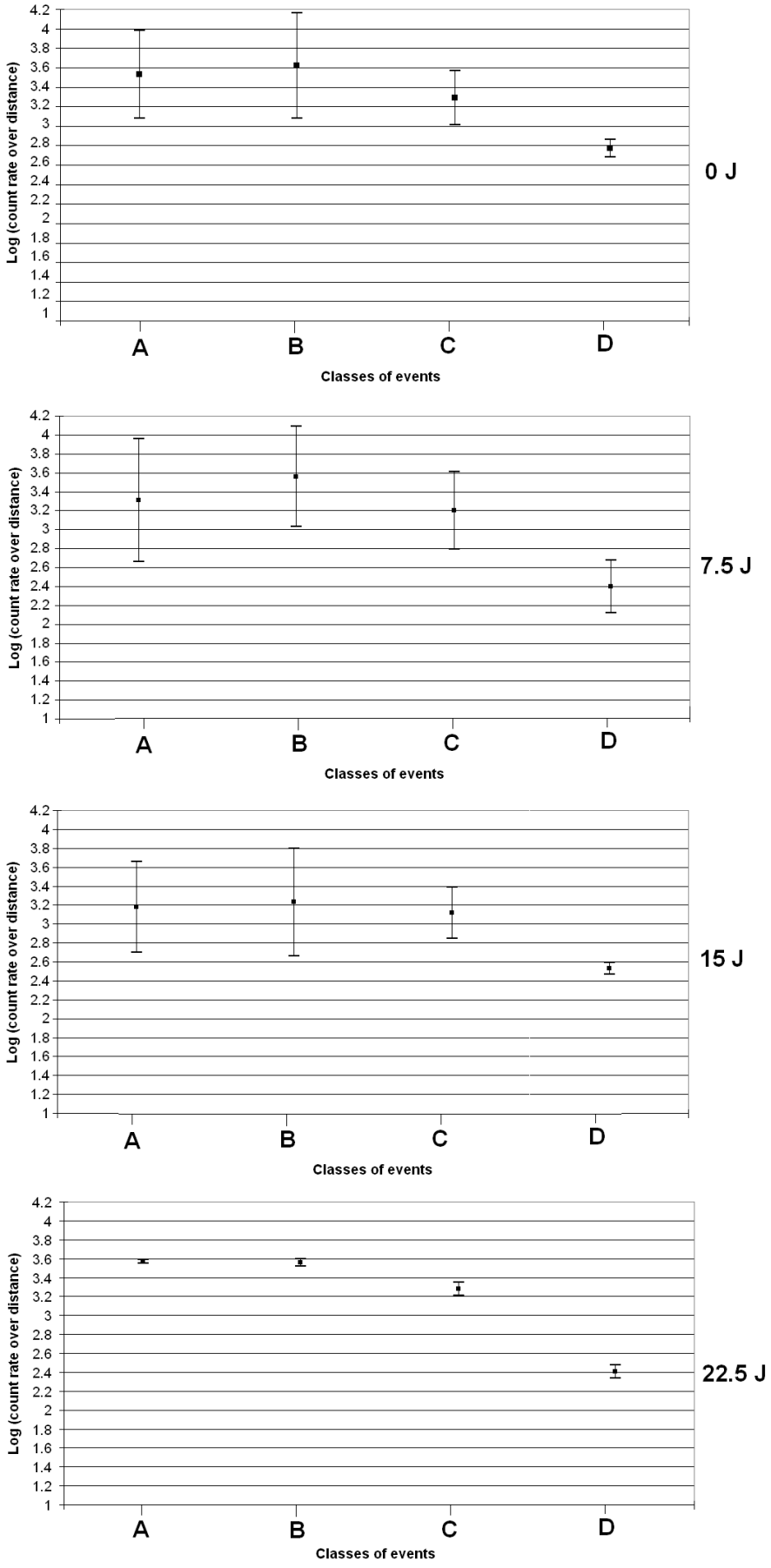

Figure 10a AE log (Count rate over distance) vs. X-location for basalt fibre reinforced laminates

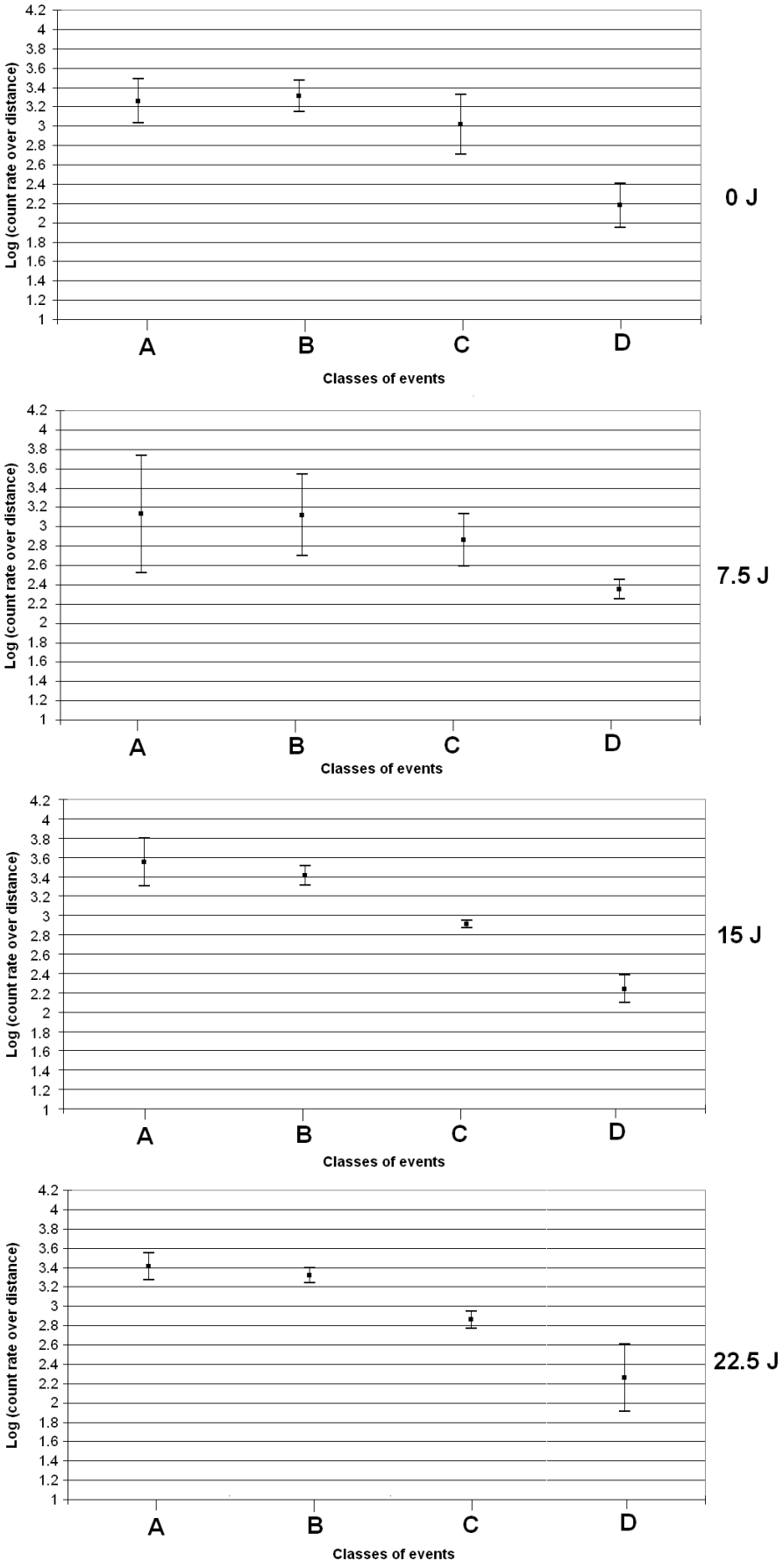

Figure 10b AE log (Count rate over distance) vs. X-location for E-glass fibre reinforced laminates

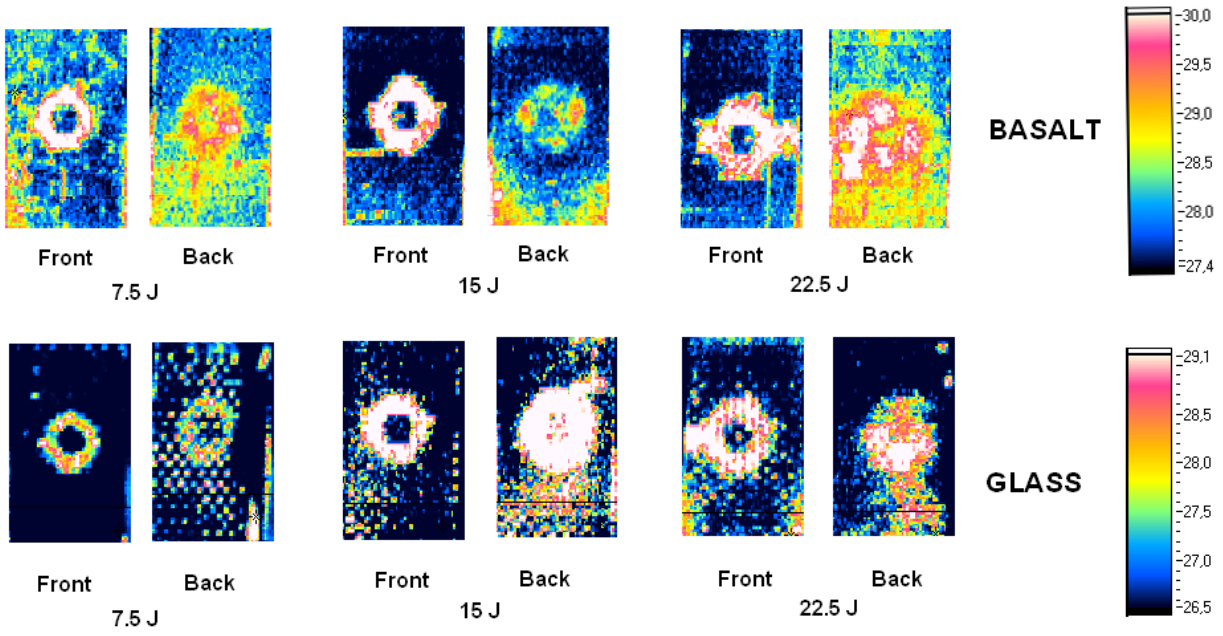

Figure 11 IR thermograms of both surfaces of the impacted laminates

Impact damage characterisation

In Figure 11 are represented the impacted and non-impacted surface of the two laminates at the different impact energies. As a general consideration, the visualisation of the impacted area was easier on the basalt fibre reinforced laminates, due to their high emissivity, whilst in some cases on the glass fibre reinforced laminates the weaving structure created some disturbance to the thermographic signal. The measurements suggest that as a whole at 7.5 and 15 J the impact damaged area is slightly higher for the basalt than for the glass fibre reinforced laminates. At 22.5 J both laminates appear heavily damaged in most of their mid-section corresponding to the impact line. However, the former laminates seem to show a more symmetrical delamination area, extending towards both edges, which is not the case for the latter. Symmetrical damage is indicative of a more homogeneous behaviour, as regards heat transmission in the sample, which may imply also a more pronounced mechanical isotropy of the laminate with respect to GFRP [21].

Whilst thermography reflects on the back surface part of the damage present inside the laminate [21], photographs with inverted value colours do give an objective picture of the presence of impact cracks on the rear surface of the basalt fibre laminates (Figure 12a). Similar images on E-glass fibre reinforced laminates (Figure 12b) do suggest that the internal delaminated area is much larger, as it is visible from the images taken at rear, although no obvious cracks are visible on the rear surface. Coming back to the results obtained earlier by examining AE localisation data, which state that the global damage produced on the two laminates by the same impact energies is quite similar, such

damage appears more concentrated in the inner part of B-area for basalt fibre reinforced lamniates, whilst it is more spread in the whole of B-area for E-glass fibre reinforced laminates.

This is substantially confirmed by SEM micrographs representing transverse sections of impacted region of both laminates, comparing images at the highest impact energy, basalt fibre laminates do show less extended cracks, whilst in glass fibre laminates they propagate in the whole of the laminate thickness (Figure 13).

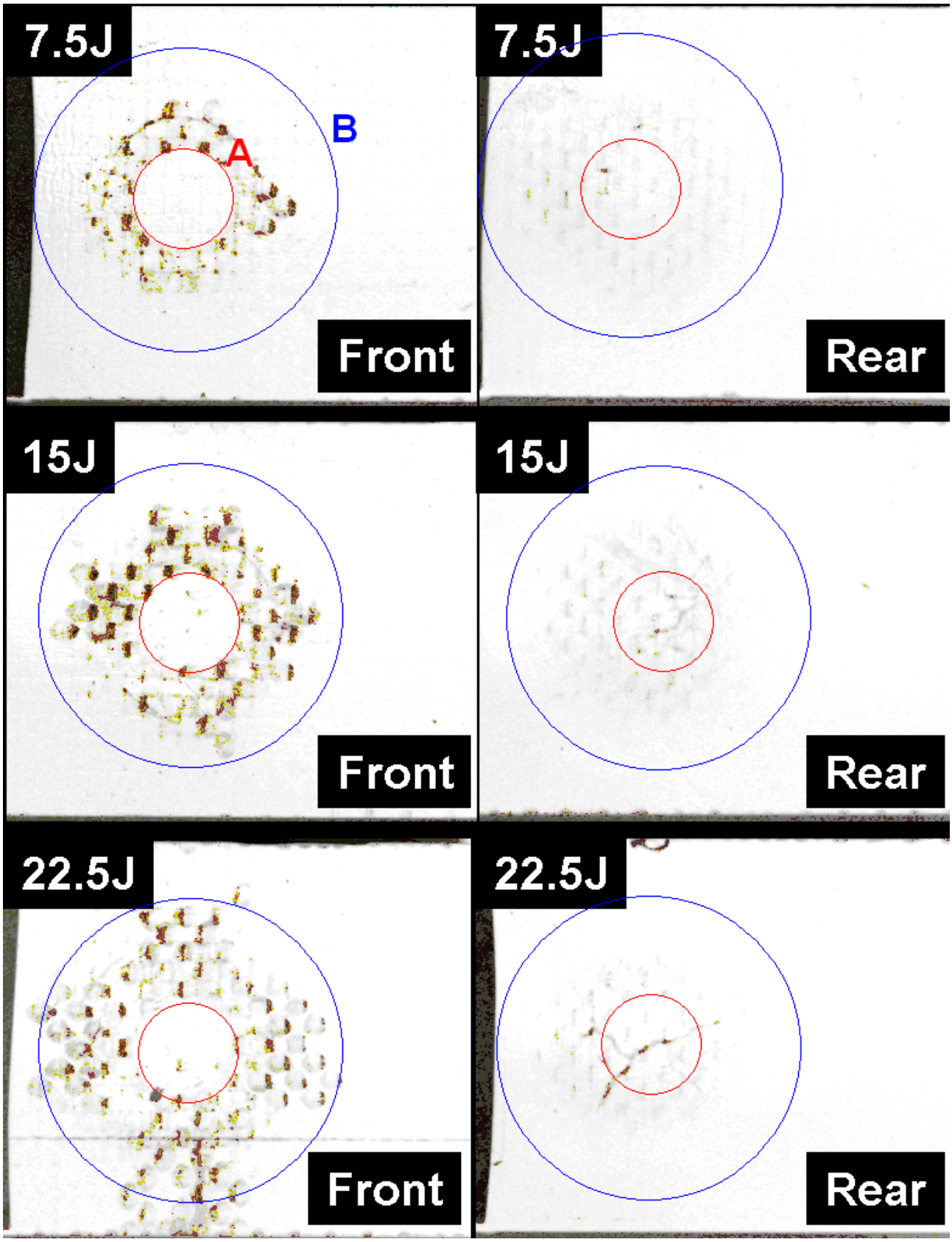

Figure 12a Inverted value photographs of impacted basalt fibre reinforced laminates

(A and B areas are as defined for AE localisation analysis)

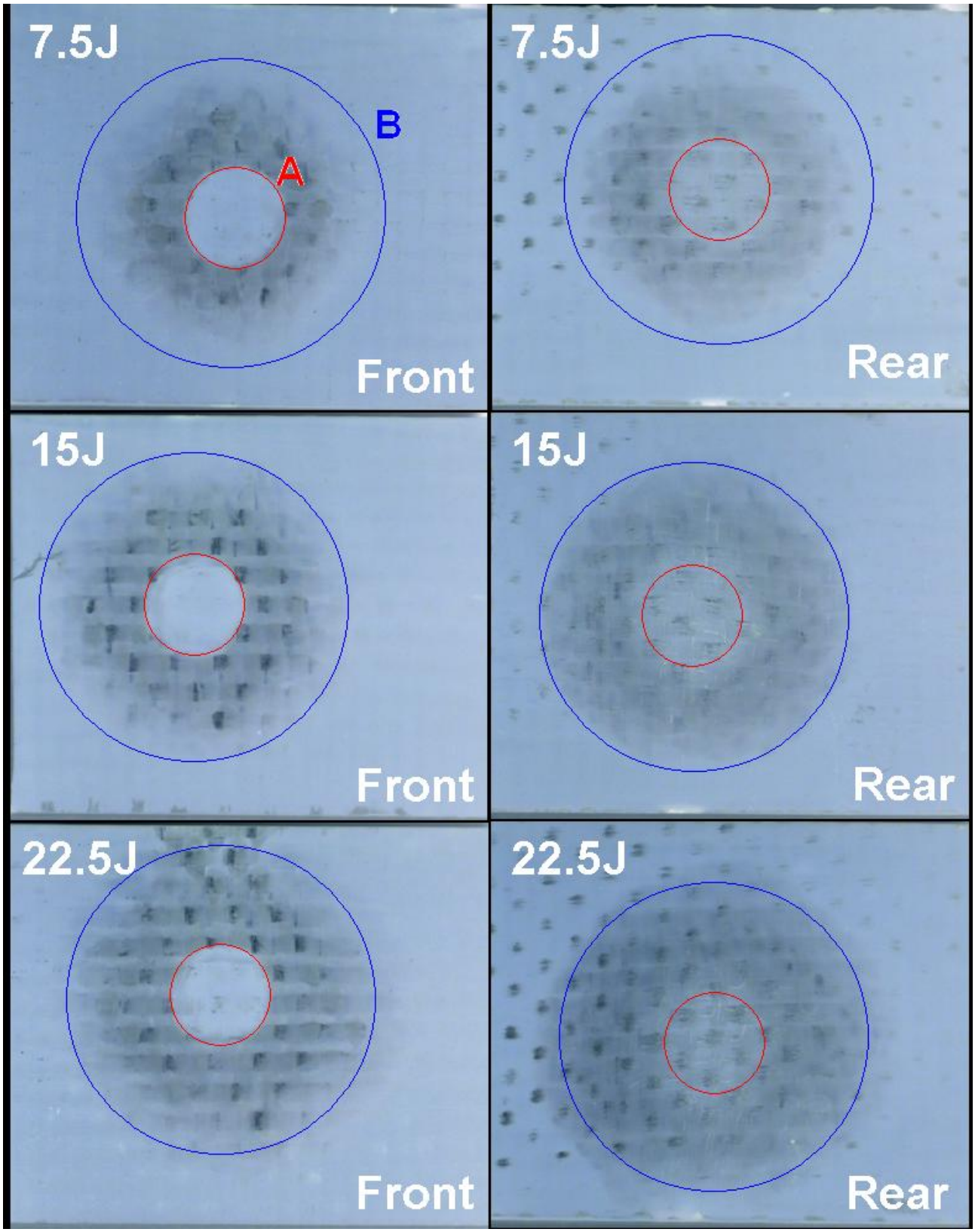

Figure 12b Inverted photographs of impacted E-glass fibre reinforced laminates

(A and B areas are as defined for AE localisation analysis)

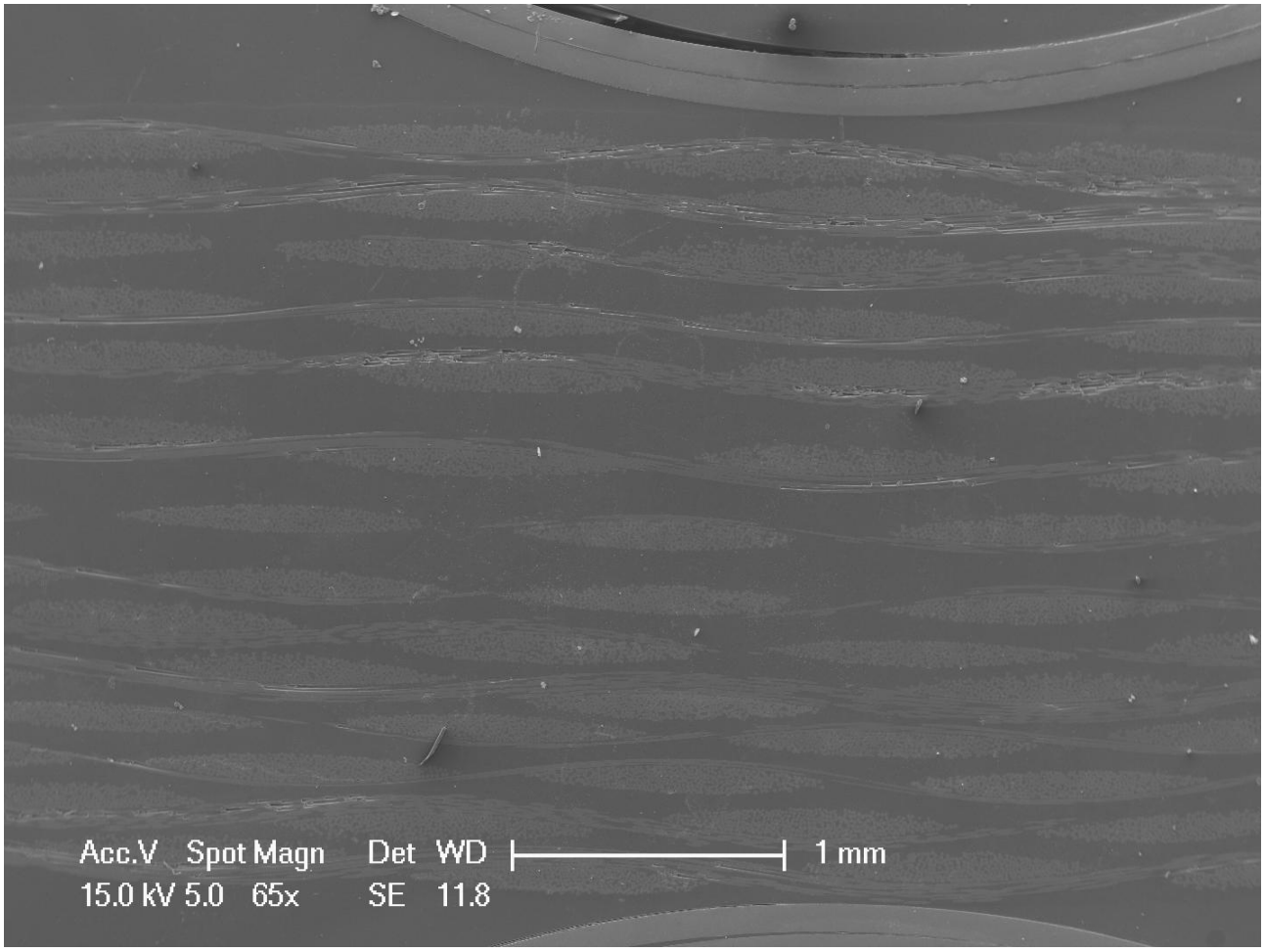

Figure 13a Transverse section of impacted surface of a basalt fibre reinforced laminate (impacted at 22.5 J)

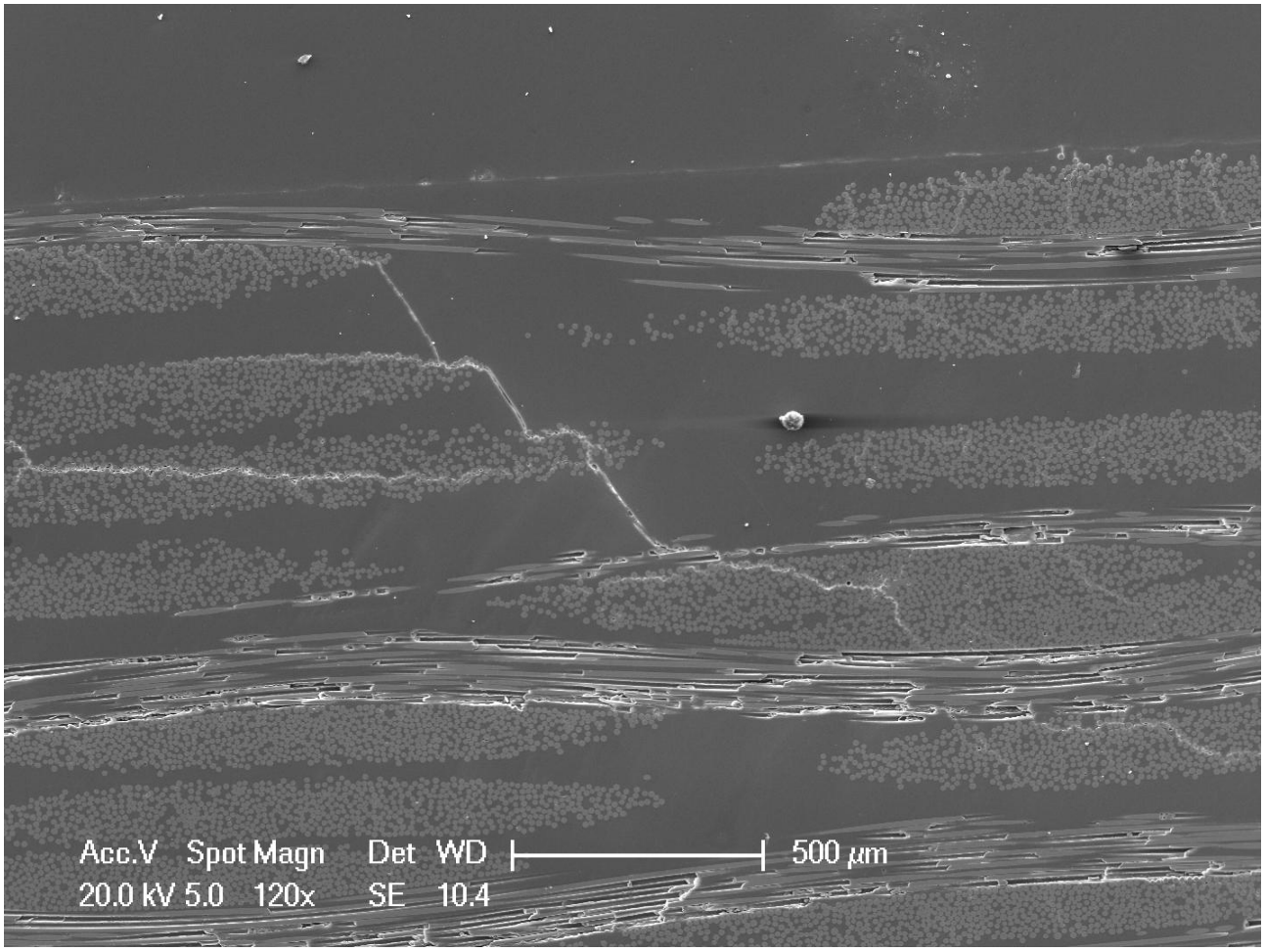

Figure 13b Transverse section of impacted surface of an E-glass fibre reinforced laminate (impacted at 22.5 J)

CONCLUSIONS

This comparative study between E-glass and basalt fibre reinforced laminates suggests that both materials have a similar damage tolerance to impact and also their post-impact residual properties after impact do not differ much, with a slight superiority for basalt fibre reinforced laminates. In general, the maximum impact energy applied, 22.5 J, does result in a degradation of flexural strength and modulus not exceeding 15%. The principal difference is represented by the presence of an extensive delamination area on E-glass fibre reinforced laminates, whilst damage appears more concentrated on basalt fibre reinforced laminates. Future studies will involve the possible preparation of hybrids between the two laminates, aimed at optimisation of their impact resistance.

REFERENCES

1. Czigány T, Trends in fiber reinforcements – the future belongs to basalt fiber. Express Polymer Letters 1, 2007, 59.

2. Deak T, Czigány T, Chemical composition and mechanical properties of basalt and glass fibers: a comparison, Textile Research Journal 2009, 79:645-651.
3. Czigány T, Vad J, Pölöskei K. Basalt fiber as reinforcement of polymer composites. Period Polytech Mech Eng 2005;49:3–14.
4. Szabó JS, Czigány T. Static fracture and failure behavior of aligned discontinuous mineral fiber reinforced polypropylene composites. Polymer Testing 2003;22:711–9.
5. Ronkay F, Czigány T. Development of composites with recycled PET matrix. Polymer Advanced Technology 2006;17:830–4.
6. Öztürk S. The effect of fibre content on the mechanical properties of hemp and basalt fibre reinforced phenol formaldehyde composites. J Mater Sci 2005;40:4585–92.
7. Czigány T. Special manufacturing and characteristics of basalt fiber reinforced hybrid polypropylene composites: mechanical properties and acoustic emission study. Composites Science and Technology 2006;66:3210–20.
8. Czigány T, Pölöskei K, Karger-Kocsis J. Fracture and failure behavior of basalt fiber mat-reinforced vinylester/epoxy hybrid resins as a function of resin composition and fiber surface treatment. Journal of Materials Science 2005;40:5609–18.
9. Mingchao W, Zuoguang Z, Yubin L, Min L, Zhijie S. Chemical durability and mechanical properties of alkali-proof basalt fiber and its reinforced epoxy composites. Journal of Reinforced Plastics and Composites 2008;27:393–407.
10. Liu Q, Shaw MT, Parnas RS, McDonnell AM. Investigation of basalt fiber composite mechanical properties for applications in transportation. Polymer Composites 2006;27:41–8.
11. Liu Q, Shaw MT, Parnas RS, McDonnell AM. Investigation of basalt fiber composite aging behavior for applications in transportation. Polymer Composites 2006;27:475–83.
12. Wittek T, Tanimoto T, Maekawa Z. Manufacture method and mechanical properties of composite material based on natural mineral fibres and biodegradable resin. Journal of Textile Engineering 2008;54:157–64.
13. Wittek T, Tanimoto T. Mechanical properties and fire retardancy of bidirectional reinforced composite based on biodegradable starch resin and basalt fibres. Express Polymer Letters 2008;2:810–22.
14. Carmisciano S, De Rosa IM, Sarasini F, Tamburrano A, Valente M, Basalt woven fiber reinforced vinylester composites: Flexural and electrical properties, Materials and Design 2011;32: 337-42.
15. Lopresto V, Leone C, De Iorio I, Mechanical characterization of basalt fibre reinforced plastic, Composites Part B (2011), in press, doi:10.1016/j.compositesb.2011.01.030.

16. Dehkordi MT, Nosraty H, Shokrieh MM, Minak G, Ghelli D, Low velocity impact properties of intra-ply hybrid composites based on basalt and nylon woven fabrics, Materials and Design 2010; 31:3835–44.
17. De Rosa IM, Santulli C, Sarasini F, Valente M, Post-impact damage characterization of hybrid configurations of jute/glass polyester laminates using acoustic emission and IR thermography, Composites Science and Technology 2009;66:1142-50.
18. De Rosa IM, Santulli C, Sarasini F, Valente M, Effect of loading-unloading cycles on impact-damaged jute/glass hybrid laminates, Polymer Composites 2009;30:1879-1887.
19. Mertiny P, Juss K, El Ghareeb MM, Evaluation of glass and basalt fiber reinforcements for polymer composite pressure piping, Journal of Pressure Vessel Technology-Transactions of the ASME 131 (6), 2009, paper 061407 (6 pp.)
20. McCartney LN, Schoeppner GA, Predicting the effect of non-uniform ply cracking on the thermoelastic properties of cross-ply laminates, Composites Science and Technology 2002;62:1841-56.
21. Meola C, Carlomagno GM, Giorleo, L, Geometrical limitations to detection of defects in composites by means of infrared thermography, Journal of Nondestructive Evaluation 2004;23:125-32.